

Fuzzy logic control for a wind/battery renewable energy production system

Onur Özdal MENGİ^{1,*}, İsmail Hakkı ALTAŞ²

¹*Giresun Technical Vocational School of Higher Education, Giresun University,
28200 Giresun-TURKEY*

e-mail: onurmengi@yahoo.com

²*Department of Electrical and Electronics Engineering, Faculty of Engineering,
Karadeniz Technical University, 61080 Trabzon-TURKEY*

e-mail: ihaltas@ktu.edu.tr

Received: 16.04.2011

Abstract

In this study, a designed proportional-integral (PI) controller and a fuzzy logic controller (FLC) that fix the voltage amplitude to a constant value of 380 V and 50 Hz for loads supplied from a wind/battery hybrid energy system are explained and compared. The quality of the power produced by the wind turbine is affected by the continuous and unpredictable variations of the wind speed. Therefore, voltage-stabilizing controllers must be integrated into the system in order to keep the voltage magnitude and frequency constant at the load terminals, which requires constant voltage and frequency. A fuzzy logic-based controller to be used for the voltage control of the designed hybrid system is proposed and compared with a classical PI controller for performance validation. The entire designed system is modeled and simulated using MATLAB/Simulink GUI (graphical user interface) with all of its subcomponents.

Key Words: *Fuzzy logic controller, proportional-integral controller, renewable energy, wind turbine*

1. Introduction

Wind energy is one of the most prominent renewable energy sources on earth. During the last decade, there has been tremendous growth in both the size and the power of wind energy converters (WECs). The global installed power increased from 7.5 GW in 1997 [1] to more than 194 GW in 2010 [2]. At the same time, turbines have grown in size, with rotor diameters of more than 100 m and power ratings ranging from kilowatts to megawatts, such as 7.5 MW. This enormous development and the more recent use of wind energy in offshore applications have led to high demands for the design, construction, and operation of WECs. Thus, a major new industry has been established and a new interdisciplinary field of research has begun to grow, affecting scientists from areas such as engineering, physics, and meteorology.

*Corresponding author: Giresun Technical Vocational School of Higher Education, Giresun University, 28200 Giresun-TURKEY

The total electricity demand in 2009 in the United States of America was 3.953×10^9 kWh. The global demand will reach 22.82×10^{12} kWh in 2015 [2]. Most of the present electricity demand in the world is met by fossil-fuel and nuclear power plants. A small part is met by renewable energy technologies, such as wind, solar, biomass, geothermal, and ocean sources. Among the renewable power sources, wind and solar energy have experienced a remarkably rapid growth in the past 10 years. Both are pollution-free sources of abundant power.

Wind power generation capacity saw an average global annual growth rate of 30% during the period from 1993 to 2003. More than 8 GW of new wind capacity was added globally in 2003, at an investment value of US\$9,000,000,000. This brought the total cumulative wind capacity to 40 GW. The most explosive growth occurred in Germany. Offshore wind farms are bringing a new dimension to the energy market. Many have been installed, and many more are being installed or are in the planning stage [3].

Energy is produced on farms composed of wind turbines. These types of systems are large power systems. For small applications, these energy types can also be used easily. For very small applications, battery groups and wind turbines can be used together [4]. For large power applications, because of the costs, battery groups cannot be used. For some houses that are farther away from the grid or obtaining energy only from renewable energy sources, however, the wind turbines and the battery groups can be used together. Diesel generators [5-8], solar panels [9,10], or fuel cells [11-13] can also be added to these systems. These systems are controlled by various control techniques. The objective of energy studies is to hold the amplitude and frequency of the voltage at a constant value. These systems can work with or without connection to the grid [14-19].

Energy is produced by wind turbines with different electric motors. These can be asynchronous motors (ASM), synchronous motors (SM), or direct-current motors (DCM) [4,20]. The voltage produced can be direct current or alternative current. In this study, a squirrel-caged ASM was used. As the ASM works freely, the reactive energy that it needs is supplied by a capacitor group [21-24].

In the literature, different controlling types of both renewable energy sources and power electronic converters can be seen [25,26]. In some research, control techniques such as fuzzy logic control [27], proportional-integral (PI)-derivative control [28], and fuzzy neural networks [29] are frequently used. The used chopper and inverter are controlled by these techniques.

In commercial products, there is a problem in holding the voltage at constant values such as 380 V and 50 Hz. At a true frequency and voltage, the loads must be supplied with a clean energy that does not contain harmonics. If not, the harmonics can cause some faults and early aging problems for the components. Researchers are therefore heavily focused on these subjects.

In this paper, the fixing of voltage amplitude at a constant value of 380 V by using a controller for the loads supplied from a wind/battery energy production system is explained. The wind speed was continuously changed and the behavior of the system was analyzed. For the controller, both a PI controller and a fuzzy logic controller (FLC) were used; the results were compared. The quality of the energy was observed by taking measurements of the loads frequently. The value of the total harmonic distortion (THD) was held at the standard intervals. The entire system and all of its subcomponents were designed in a MATLAB/Simulink environment.

2. Wind/battery energy production system

The overall system structure, consisting of a 3-phase load, wind/battery hybrid energy system, interfacing converters, filters, and control unit, is shown in Figure 1. When the wind speed is sufficient, the whole system is supplied by the wind turbine; otherwise, the batteries are turned on to supply the system. The direct-current (DC) voltage produced by the wind/battery system is converted to alternative-current (AC) voltage using a 3-phase inverter in order to supply power to the 3-phase load. The voltage output of the inverter is controlled to keep the voltage at 380 V, line to line, at a fixed frequency of 50 Hz. The 3-phase voltages are converted to d-q axis layouts as direct-axis voltage V_d and quadrature voltage V_q , to be used by the PI controller and the FLC. The output of the controller is then used to generate a pulse-width modulated (PWM) signal, which is used to control the output voltage of the inverter. The frequency of the inverter is controlled and kept constant at 50 Hz through a phase-locked loop (PLL) process.

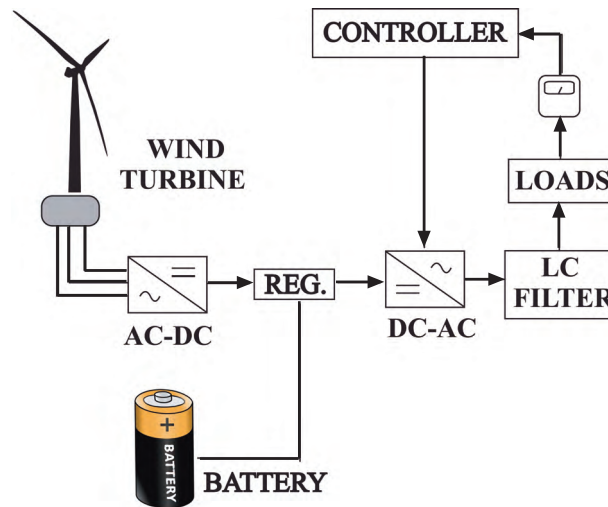


Figure 1. PV/battery renewable source.

The filters in the system are used to supply clean AC voltage to the loads. The value of the THD in the system was measured and compared with the correct standard values.

All of the subsystem components (wind turbine, batteries, FLC, PI controller, inverter, 3-phase load, regulator, and filters) were submodeled individually using the MATLAB/Simulink GUI (graphical user interface) environment and were combined to establish the overall system model. The simulation of the proposed scheme was done in MATLAB/Simulink/SimPower to establish model validation and component compatibility.

The used regulator is a device that measures the wind speed. This controller is a mechanism that uses an on-off control technique. When the wind speed is less than a specific value, it cannot supply the guaranteed power to the system; the system then turns off the wind turbine and turns on the batteries.

In this study, a wind/battery system supplying power to 3-phase AC loads was examined. To fix the voltage on the loads at 380 V, both a PI controller and a FLC were used, and the results were compared.

2.1. The wind turbine model

Wind turbines convert mechanical energy produced by the wind to electrical energy. To use this electrical energy, voltage and frequency regulation are needed. The model of a wind turbine is developed on the basis of the steady-state power characteristics of the turbine. The mechanical power produced by a wind turbine is shown in Eq. (1). The Simulink model of the studied wind turbine is shown in Figure 2.

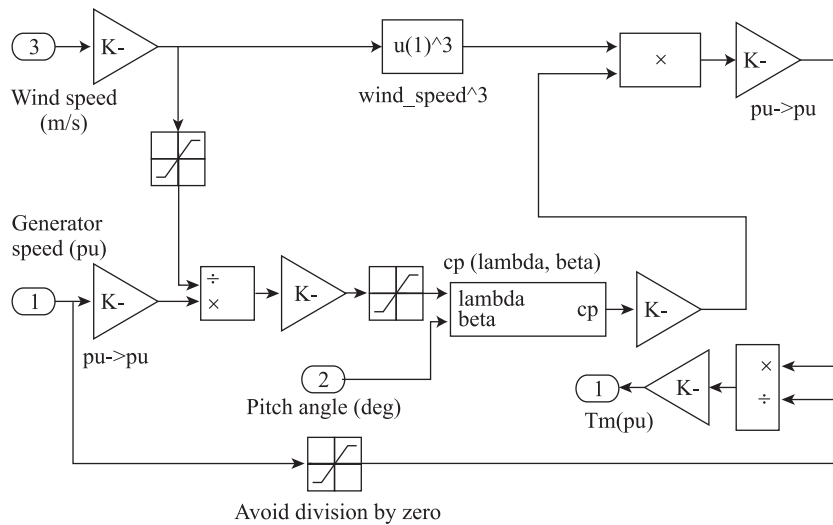


Figure 2. Wind turbine model.

$$P_m = \frac{1}{2} C_p(\lambda, \beta) \rho A v^3 \tag{1}$$

In Eq. (1), P_m is the mechanical output power of the turbine (W), C_p is the performance coefficient of the turbine, λ is the tip speed ratio of the rotor blade tip speed to the wind speed (in degrees), β is the blade pitch angle (in degrees), ρ is the air density (kg/m^3), A is the turbine swept area (m^2), and v is the wind speed (m/s). The expression “ $C_p(\lambda, \beta)$ ” is calculated by using Eqs. (2) and (3).

$$C_p(\lambda, \beta) = C_1 \left(\frac{C_2}{\lambda_1} - C_3 \beta - C_4 \right) e^{\frac{C_5}{\lambda_1}} + C_6 \lambda \tag{2}$$

$$\frac{1}{\lambda_i} = \frac{1}{\lambda + 0,08\beta} - \frac{0,035}{\beta^3 + 1} \tag{3}$$

Coefficients C_1 through C_6 are: $C_1 = 0.5176, C_2 = 116, C_3 = 0.4, C_4 = 5, C_5 = 21$, and $C_6 = 0.0068$. β is equal to 0, but, if necessary, this value can be changed [3,4].

2.2. The battery model

The nickel-metal hydride battery was modeled using a simple controlled voltage source in a series with constant resistance, as shown in Figure 3. This model assumes the same characteristics for the charge and the discharge cycles. The open voltage source was calculated with a nonlinear equation based on the actual state of charge (SOC) of the battery.

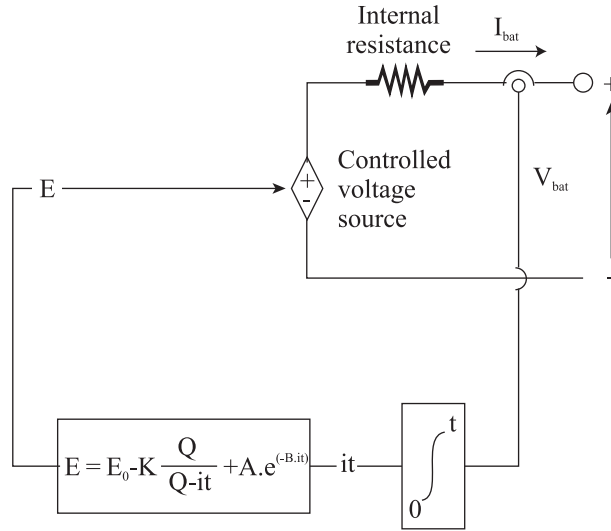


Figure 3. Nonlinear battery model.

The controlled voltage source is described by Eq. (4).

$$E = E_0 - K \frac{Q}{Q - \int_0^t i dt} + A e^{(-B \int_0^t i dt)} \quad (4)$$

Here, E is the no-load voltage (V), E_0 is the battery constant voltage (V), K is the polarization voltage (V), Q is the battery capacity (Ah), A is the exponential zone amplitude (V), B is the exponential zone time constant inverse (Ah) - 1, V_{batt} is the battery voltage (V), R is the internal resistance (Ω), i is the battery current (A), and $\int i dt = e$ actual battery charge (Ah) [28,30].

2.3. Control systems

Systems in the energy industry need to be controlled. Each system works with some rules, and these rules determine the system's instant situation. For example, in a system in which the speed is controlled, the speed data of the motor shaft are compared to the reference data, and, according to the rules, the power of the motor can be increased or decreased. In this situation, a controller is required.

2.3.1. Proportional-integral-derivative controller

Proportional-integral-derivative (PID) controllers are the most commonly used controllers, especially in the electronics industry. The basic form of the controlled systems is shown in Figure 4. The expression at the continuous time and the transfer function of the PID type of controller that is used in this system are shown in Eqs. (5) and (6) [31]. A PI type of controller is used in the simulated system.

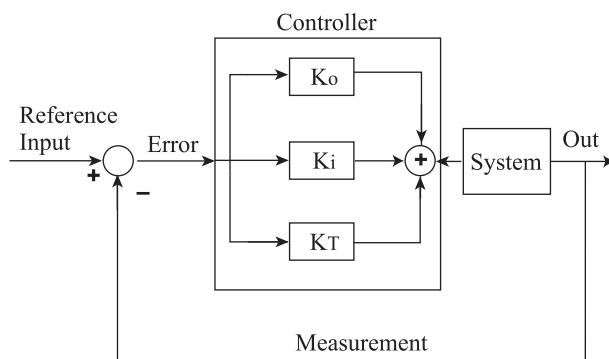


Figure 4. A system with PID controller.

$$u(t) = K_p[e(t) + \frac{1}{T_i} \int_0^t e(t)dt + T_d \frac{e(t)}{dt}] \tag{5}$$

$$G_{\text{Controller}} = K_D + K_T s + \frac{K_i}{s} \tag{6}$$

2.3.2. Fuzzy logic controller

In the energy industry, while controlling a system, it is expected that the stability and safety of the system will be assured. The system must also be cheap, easy to use, understandable, repairable, and changeable, and, above all, must increase the performance to the desired level. To achieve all of these goals, the structure and the dynamic properties of the system that will be controlled must be known and must also be mathematically modeled. Sometimes, however, due to some nonlinear systems, mathematic models are not possible. Even if the modeling is done, the controller that will be used in that system might cause some design problems and high costs. Therefore, the controller might not work at the desired performance level. In situations like this, an expert’s information is utilized. The expert presents the information and experiences as fuzzy or uncertain types to do the controlling. These characterizations are transferred to the computer, ending the need for the expert. The differences among the controls of different experts also come to an end, and the controlling of the system thus becomes flexible.

The term “fuzzy logic” can be explained as a method that utilizes the experiences of people for numerical expressions, instead of verbal and symbolic expressions, to produce the functional rules of a system. Fuzzy logic is established based upon the logical relations. In daily life, the terms that are used usually have a fuzzy structure type. While explaining something or giving an order, the terms that we use are fuzzy. Verbal terms including “old,” “young,” “tall,” “short,” “hot,” “cold,” “warm,” “cloudy,” “partly cloudy,” “sunny,” “fast,” “slow,” “a lot,” “a few,” “some,” and “more” can be understood as fuzzy variables. While people are explaining events or describing a subject, they use expressions that do not contain certainty. According to a person’s age, he is called “old,” “middle-aged,” “young,” “very old,” or “very young.” According to the slipperiness and the slope of a road, the gas and the brake pedal of a car are pushed more slowly or more quickly. If the light in a room is not sufficient, it is increased; if the light is too bright, then it is decreased. All of these situations are examples of how a human brain explains behaviors and its assessments of some situations with unclear and uncertain terms.

After the development of fuzzy logic and the publication of an article about the theory of fuzzy sets using these logic rules [32], investigations of systems containing uncertain terms showed new trends. Though developed in 1965, the term “fuzzy sets” began to be commonly used in the mid-1970s. After the mid-1980s, the usage of fuzzy logic accelerated as Japan began to use the fuzzy logic technique in various products. Today, it has reached its peak, and it is possible to find an application of fuzzy logic almost everywhere.

The general properties of fuzzy logic, as explained by Zadeh [32], are as follows. In fuzzy logic, instead of consideration based on exact data, approximate consideration is used. In fuzzy logic, all data are shown as values between 0 and 1. The information in fuzzy logic is verbal, such as “big,” “small,” “more,” or “few.” The fuzzy implication process is conducted according to rules that are defined between the verbal expressions. Every logical system can be defined as fuzzy. Fuzzy logic is very suitable for systems whose mathematical models are hard to develop. Fuzzy logic has the ability of processing uncertain or incomplete information [32,33].

The flow chart of a FLC is shown in Figure 5.

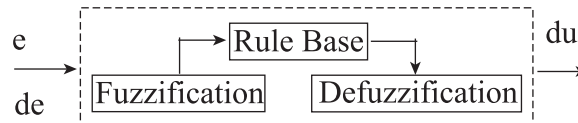


Figure 5. Basic configuration of a FLC.

As shown in Figure 5, the FLC system consists of 3 components. These are fuzzification, the rule base, and defuzzification. Fuzzification, the first component of the FLC, converts the exact inputs to fuzzy values. These fuzzy values are sent to the rule-base unit and processed with fuzzy rules, and then these derived fuzzy values are sent to the defuzzification unit. In this unit, the fuzzy results are converted to exact values.

The FLC’s input values are generally the control error and the variation of this error in one sampling time. According to these variables, a rule table is produced in the FLC’s rule-base unit.

The holding of the voltage and the amplitude of the load at the desired values of 380 V and 50 Hz is done by the FLC. The 3-phase voltage is transferred from the a-b-c axes to the d-q axes first. The voltage divides into its components, which are controlled separately. At the output of the control, the voltage is transferred in reverse, from the d-q axes to the a-b-c axes, and, at the end, the PWM is driven by that voltage. These controls are done in the regulator block.

In Figures 6 and 7, the error and the error variation of the input data of the FLC’s input variables are shown. Triangle membership functions were used. These functions are called NB, NK, S, PK, and PB, and the data vary between -1 and 1 , as seen in the Figures.

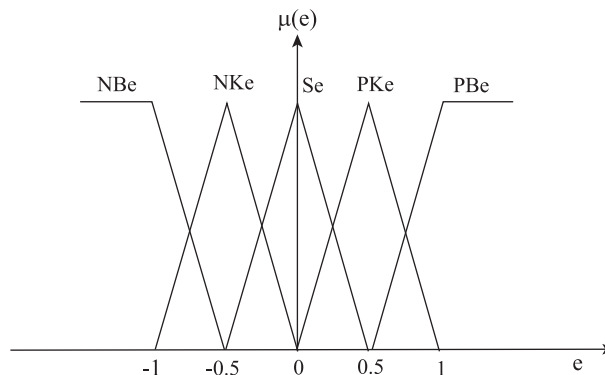


Figure 6. Error membership functions.

In Figure 8, the output space of the FLC is shown. These data also vary between -1 and 1 .

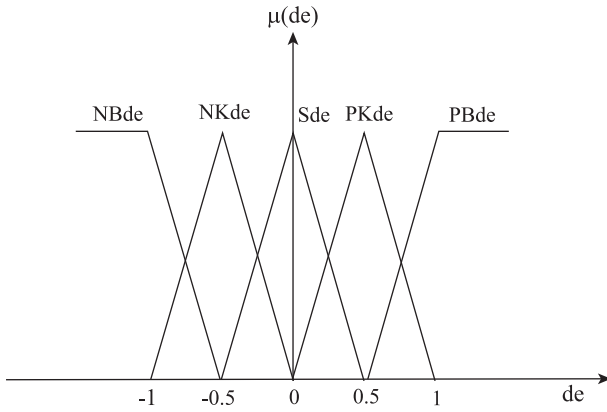


Figure 7. Variation of error membership functions.

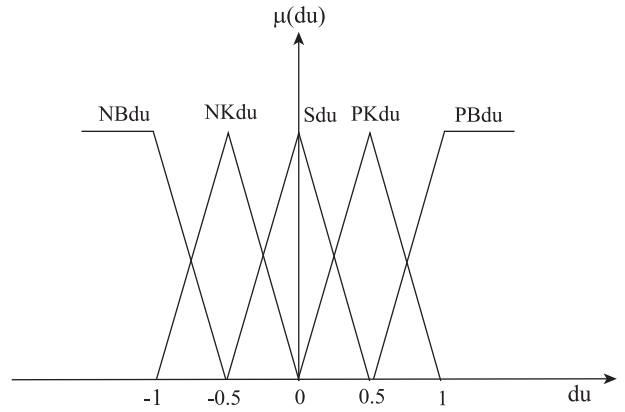


Figure 8. Output space.

These subsystems are shown in Figures 9-13. The triangle membership function is defined in Eq. (7), and its Simulink subsystem is shown in Figure 9.

$$\mu_{MU}(x) = \max \left(\min \left(\frac{x - x_1}{x_T - x_1}, \frac{x_2 - x_1}{x_2 - x_T} \right), 0 \right) \quad (7)$$

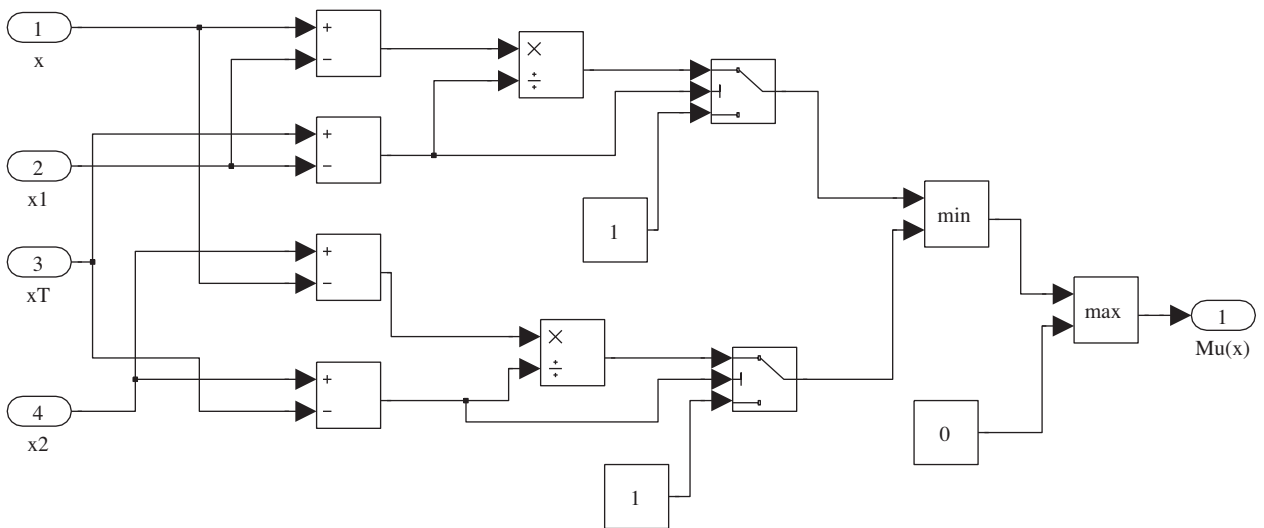


Figure 9. Triangular membership function.

In Figure 10, the fuzzification unit is shown. It is designed to be 5-ruled. The minimums of the error and its variations according to the input variables are calculated here.

In the Table, the rules of the FLC are given. Due to the 5-ruled input variables, there are 25 rules in total. The unit for the rule processing is seen in Figure 11.

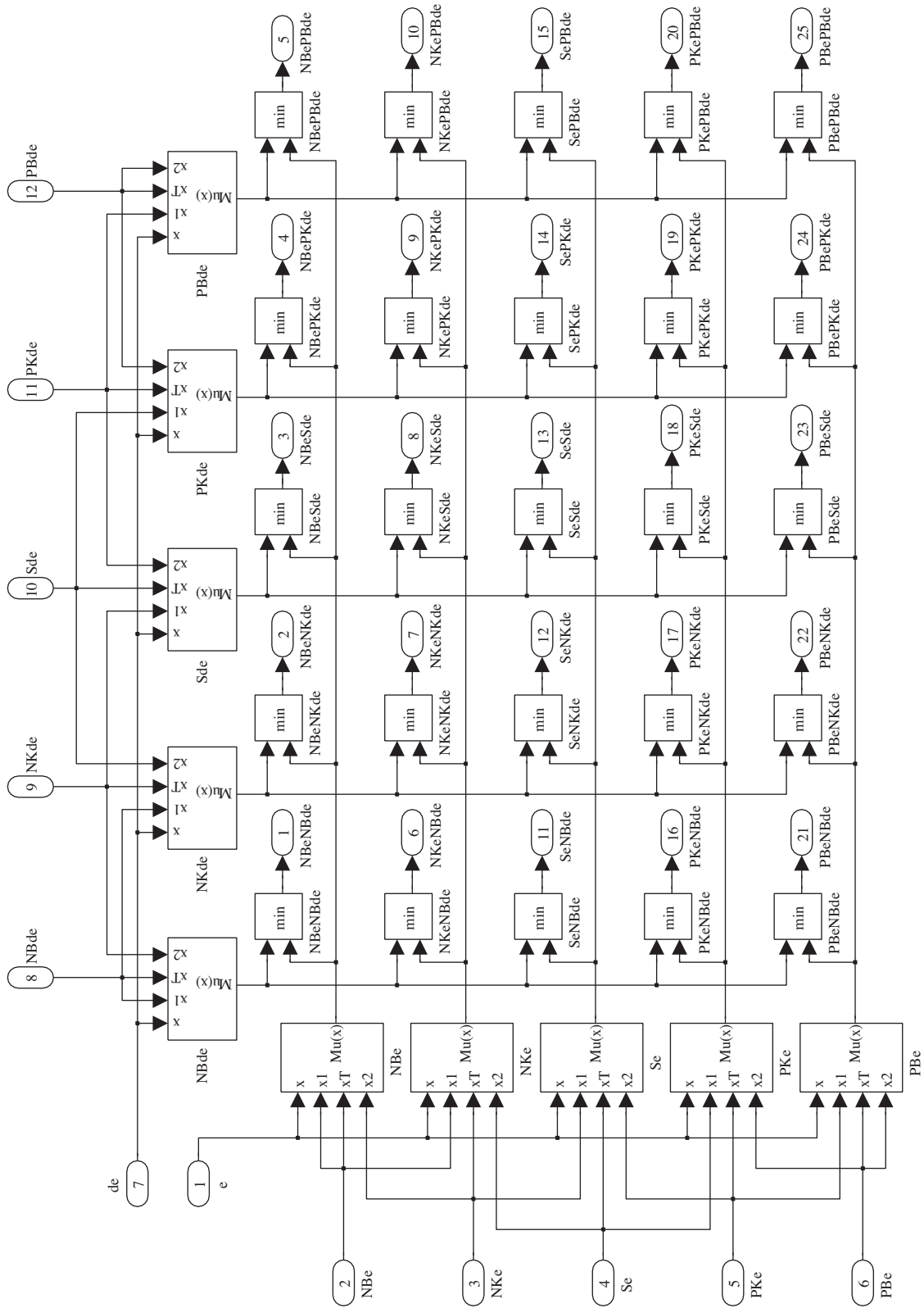


Figure 10. Fuzzification unit.

Table. Fuzzy rules.

| e / de | NB | NK | S | PK | PB |
|--------|----|----|----|----|----|
| NB | NB | NB | NK | NK | S |
| NK | NB | NK | NK | S | PK |
| S | NK | NK | S | PK | PK |
| PK | NK | S | PK | PK | PB |
| PB | S | PK | PK | PB | PB |

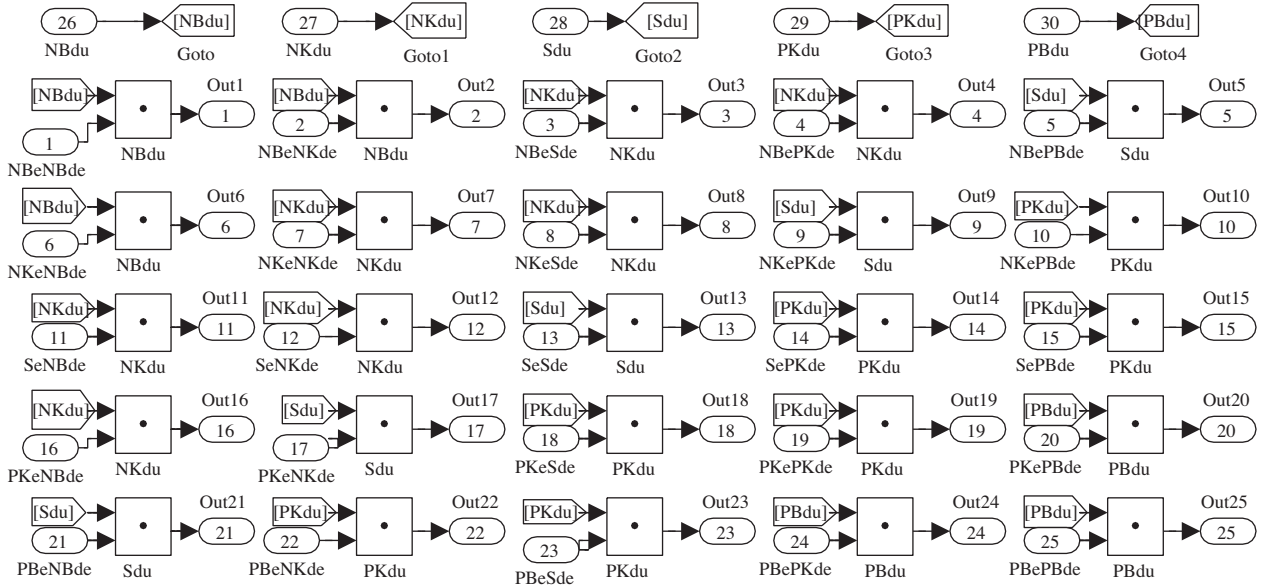


Figure 11. Fuzzy rules in Simulink.

In Figure 12, certain variables are obtained with defuzzification by using the center of the area method. In Eq. (8), the mathematical expression of this method is shown.

$$z_0 = \frac{\sum_{j=1}^n \mu_C(z_j) \cdot z_j}{\sum_{j=1}^n \mu_C(z_j)} \quad (8)$$

The designed FLC was redesigned in the MATLAB/Simulink environment, as shown in Figure 13. The user can thereby use the controller more efficiently and can establish the necessary settings easily [28].

3. Simulation system

The wind turbine is affected by the wind speed. The variations of the wind speed are shown in Figure 14. The simulated system is shown in Figure 15.

The system includes a 60-kW wind turbine and induction machine, a 55-kW battery, a regulator, an inverter, filters, a total 50-kW load, measuring units, switches, and controllers. During the simulation process, the voltages on the loads are fixed at the values of 380 V and 50 Hz.

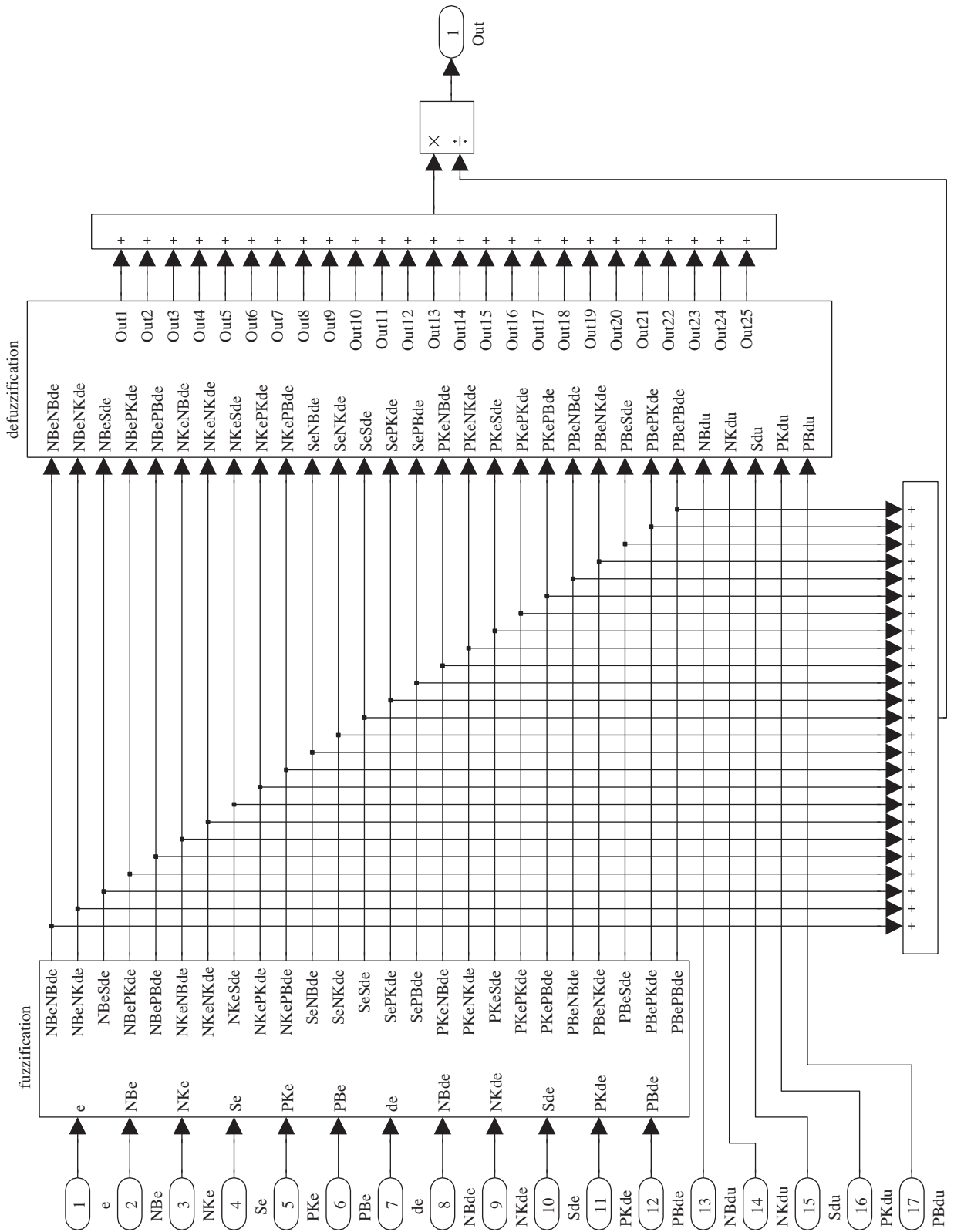


Figure 12. Defuzzification units.

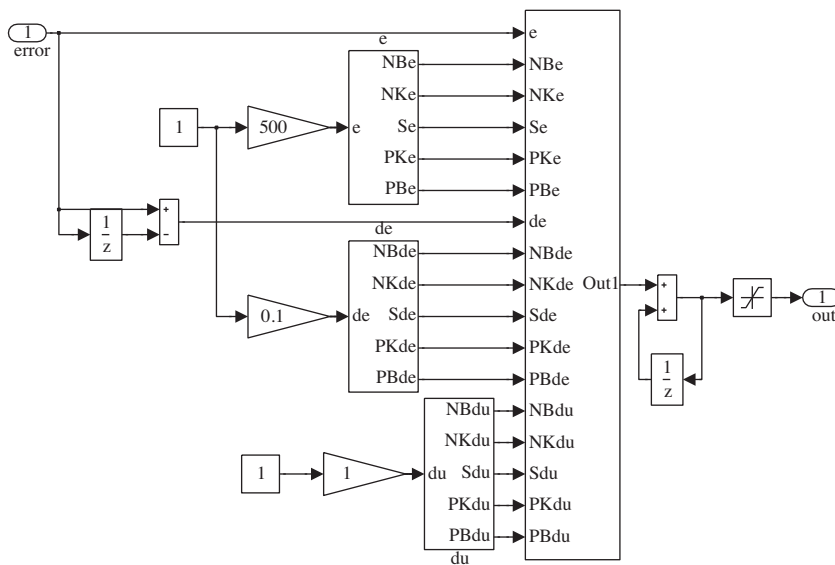


Figure 13. FLC with input and output values.

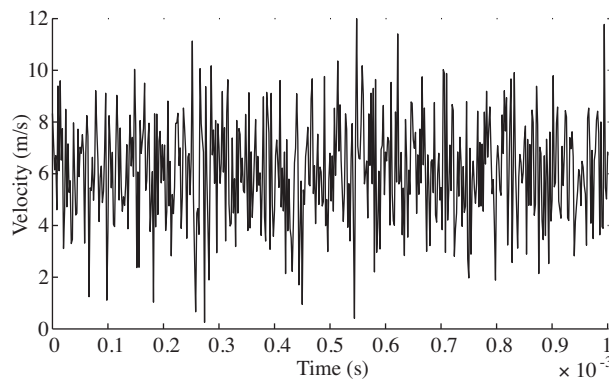


Figure 14. Variations of wind speed between 0 and 1 ms.

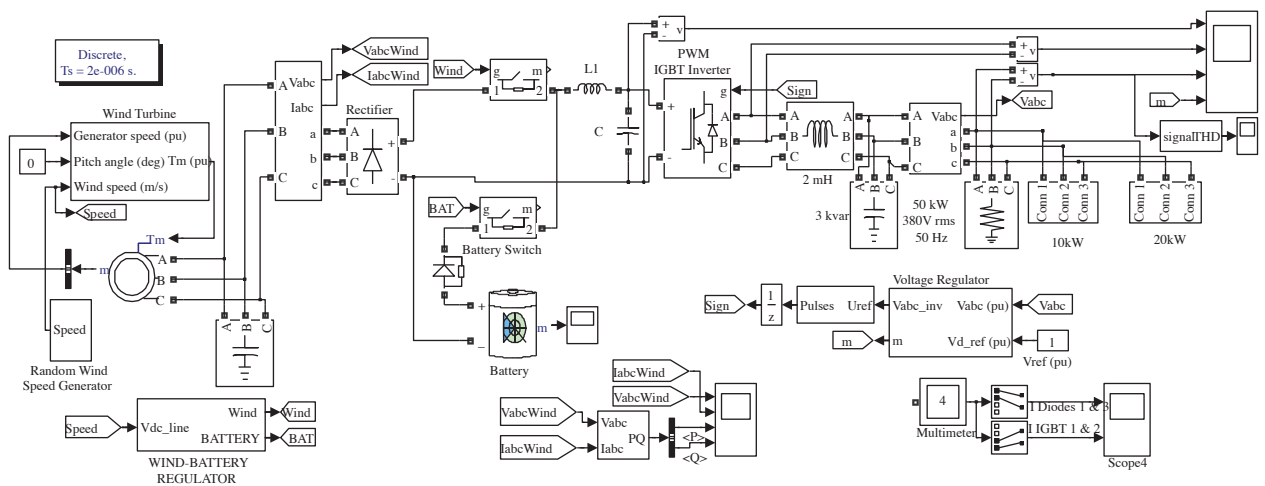


Figure 15. Main system.

The PWM used in the system's inverter has a 2-kHz switching frequency. Therefore, in the simulation, discrete time control is done at a sampling time of $2 \mu\text{s}$.

In Figure 15, the alternative voltage obtained from the wind turbine is converted to direct current by passing it through a rectifier and then filtering it. The direct current is also connected to the battery unit. It is converted to the 3-phase voltage by an inverter and then filtered again, and the loads are supplied by this voltage. To investigate the system's behavior at different loads, first a 10-kW and then a 20-kW load is added to the 20-kW reference load. The total load is 50 kW. In the system, the regulator decides when the loads will be supplied by the wind turbine or by the battery unit. According to the decision, the signals are sent to the switches that turn on and off the wind turbine and the battery unit. This process is conducted in the wind-battery block.

The voltage regulator block is the place where the control process occurs. Here, as explained before, the transfer process is done from the a-b-c axes to the d-q axes. The voltage is divided into its d and q components, which are controlled separately, and, in the output of the controller, these data are converted to the a-b-c axes from the d-q axes. The PWM is driven by that voltage.

By taking some measurements from every point, data about the system's current, voltage, and power can be examined. By changing the wind speed between 0 and 12 m/s, a simulation close to reality is undertaken.

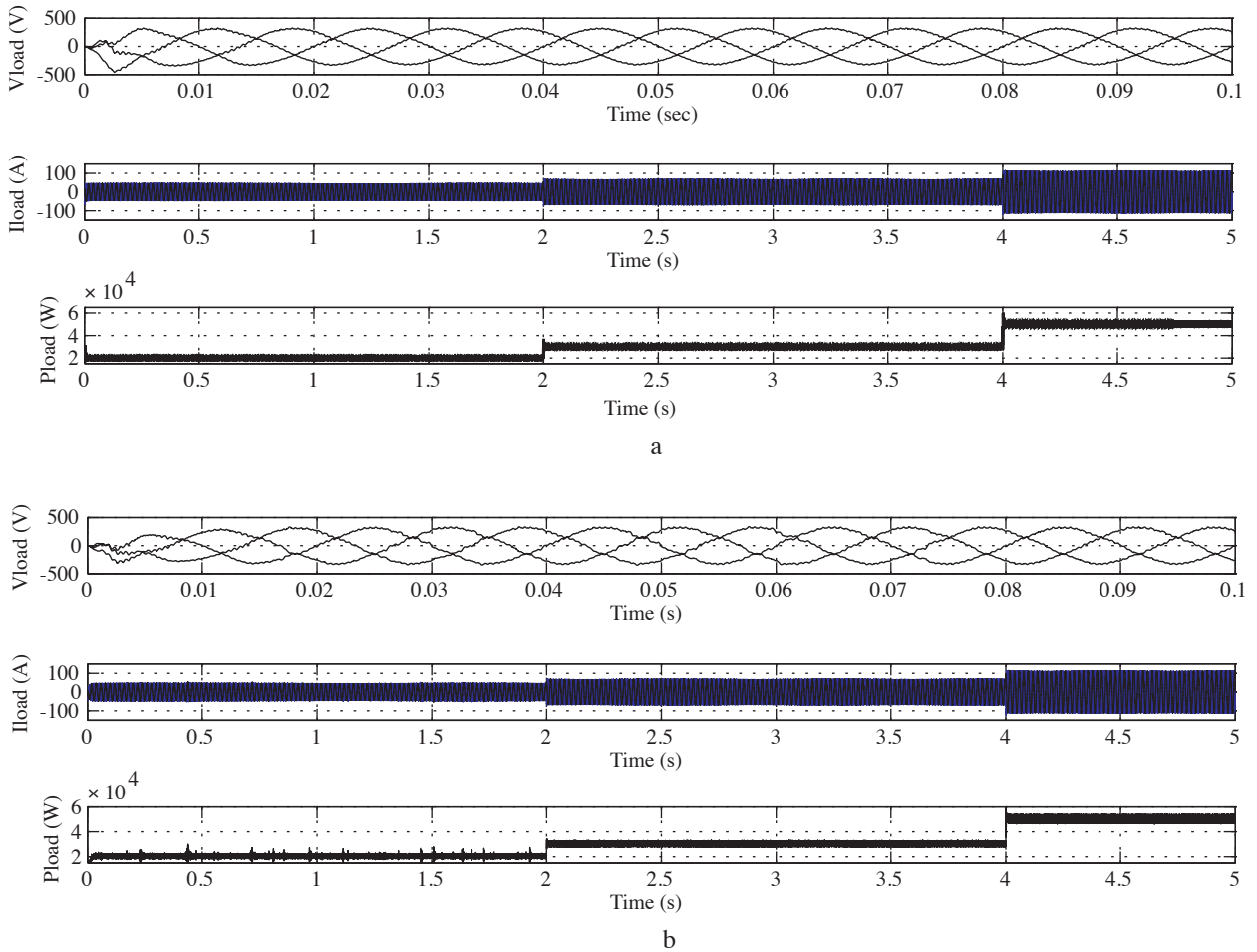


Figure 16. Power on the load: a) with a PI controller and b) with a FLC.

4. Discussion and result analysis

In Figures 16a and 16b, the active power, current, and voltage on the load with both a PI controller and a FLC are shown. The increase of the loads can be seen clearly. First a 20-kW, then a 10-kW, and finally a 20-kW load were added to the system. As a result, a total load of 50 kW is supplied by the system.

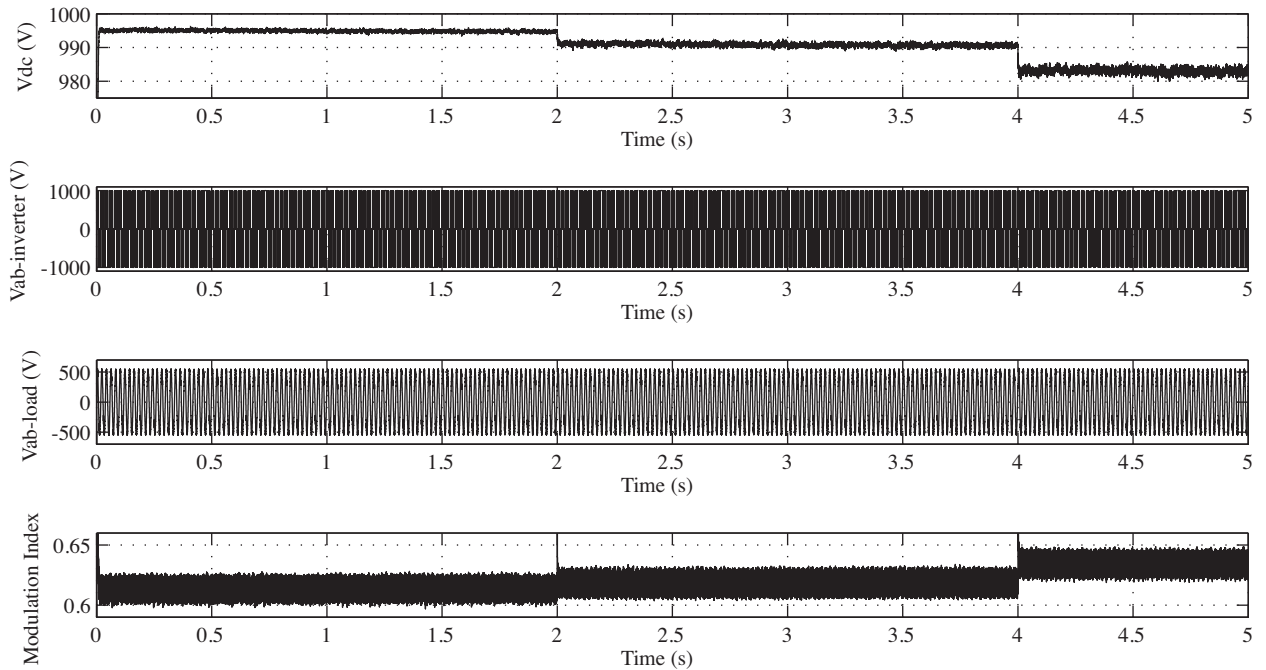


Figure 17. Results of the PI controller.

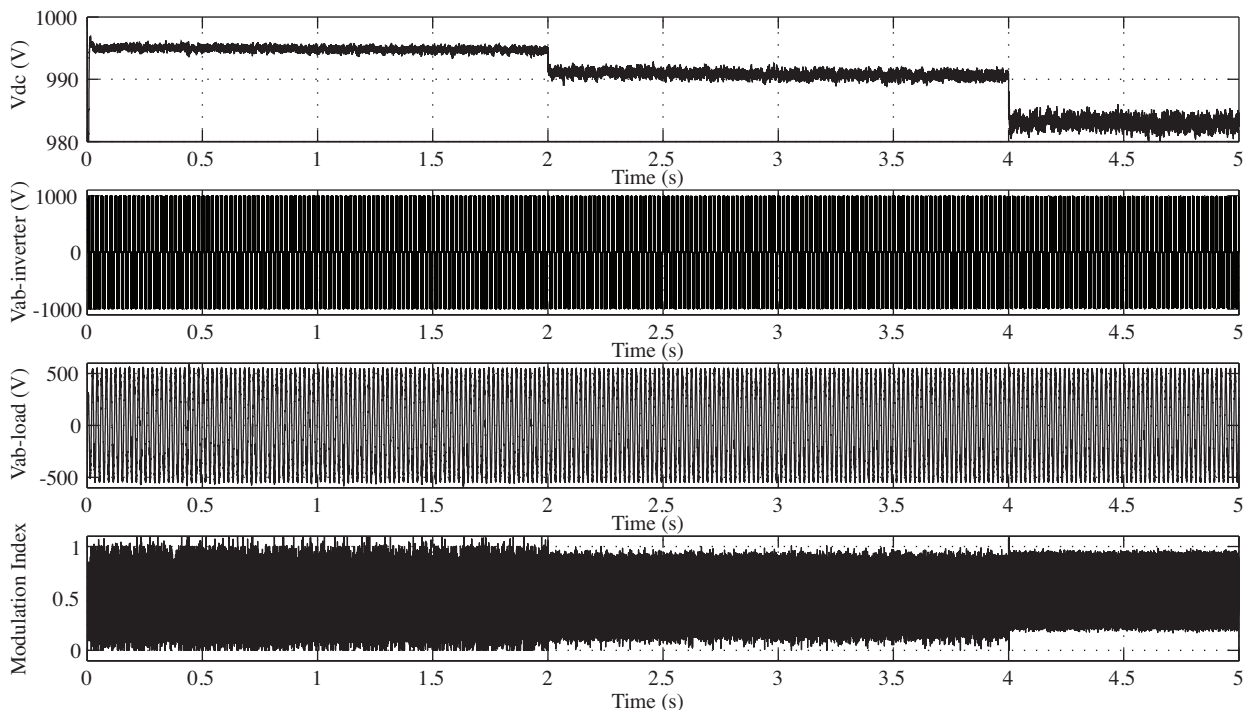


Figure 18. Results of the FLC.

In Figures 17 and 18, the results derived from the control achieved by using the PI controller and the FLC, respectively, are shown, along with the DC output voltage, the inverter's output voltage between the a and b phases, the load voltage between the a and b phases, and the variation of the modulation indexes.

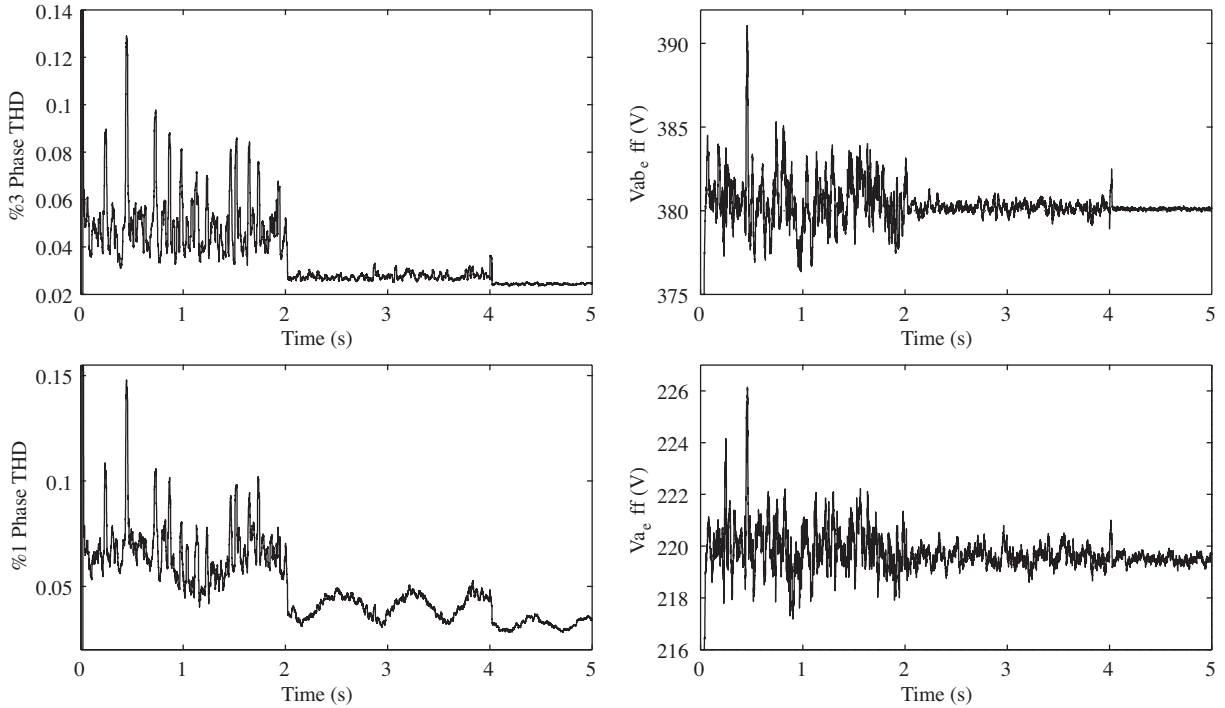


Figure 19. PI controller results.

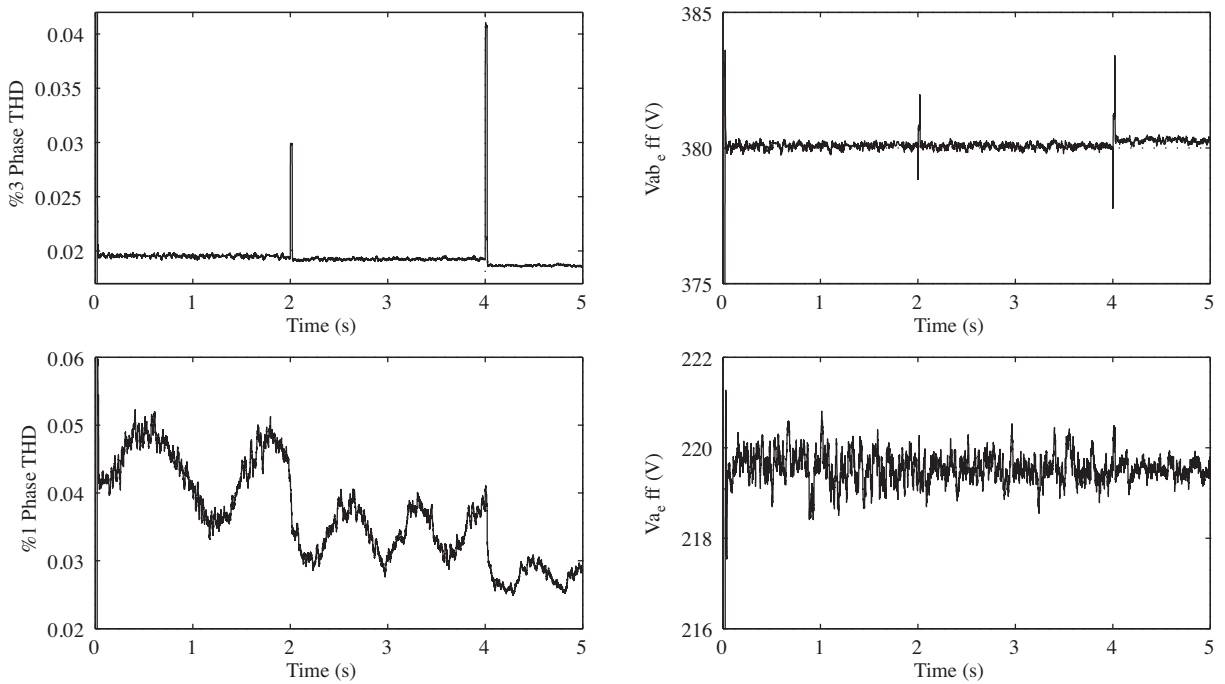


Figure 20. FLC results.

In Figure 19, the voltage on the load reaches a value of 380 V at 2 s with the PI controller. The maximum overshoot voltage that can be reached is 392 V. The 3-phase THD value is less than 10% at the steady situation. In Figure 18, the results derived from the control done by using the FLC are shown, along with the DC output voltage, the inverter's output voltage between the a and b phases, the load voltage between the a and b phases, and the variation of the modulation indexes. The voltage on the load reaches a value of 380 V at 0.05 s with the FLC. The maximum overshoot value is 384 V. The 3-phase THD value is less than 2% at the steady situation. Detailed results are shown in Figures 19 and 20.

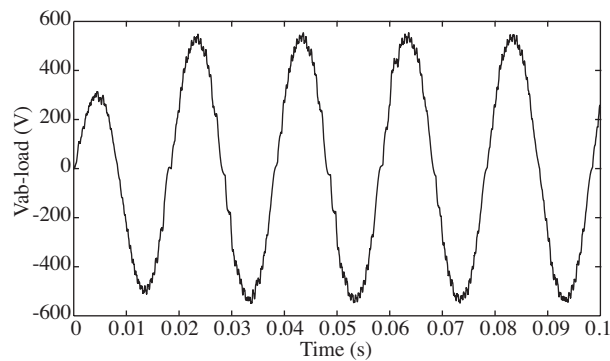


Figure 21. $V_{ab-load}$ variation for PI controller.

In Figures 21 and 22, the variation of the voltage between the a and b phases done in simulations with the PI controller and FLC in sequence are shown. As can be seen from the THD values, the FLC has a less harmonic and a clean sinus wave.

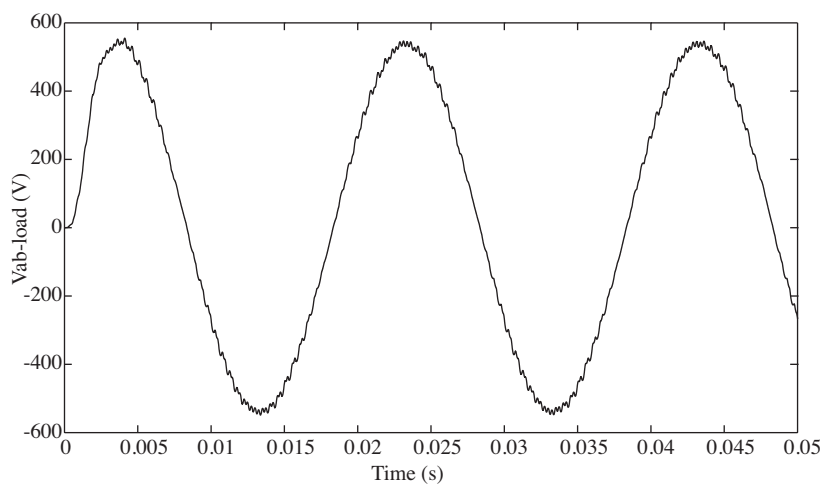


Figure 22. $V_{ab-load}$ variation for the FLC.

In Figures 23 and 24, the variations of the electrical parameters of the wind turbine are shown.

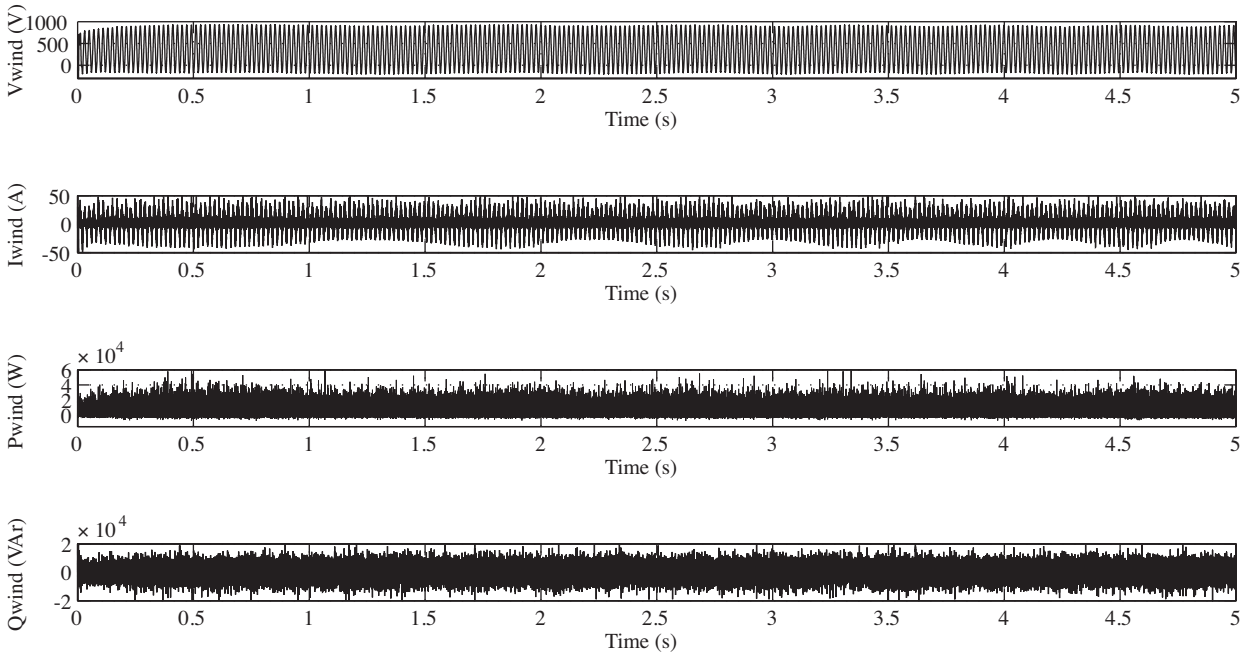


Figure 23. Wind turbine V, I, active, and reactive power variations with PI system.

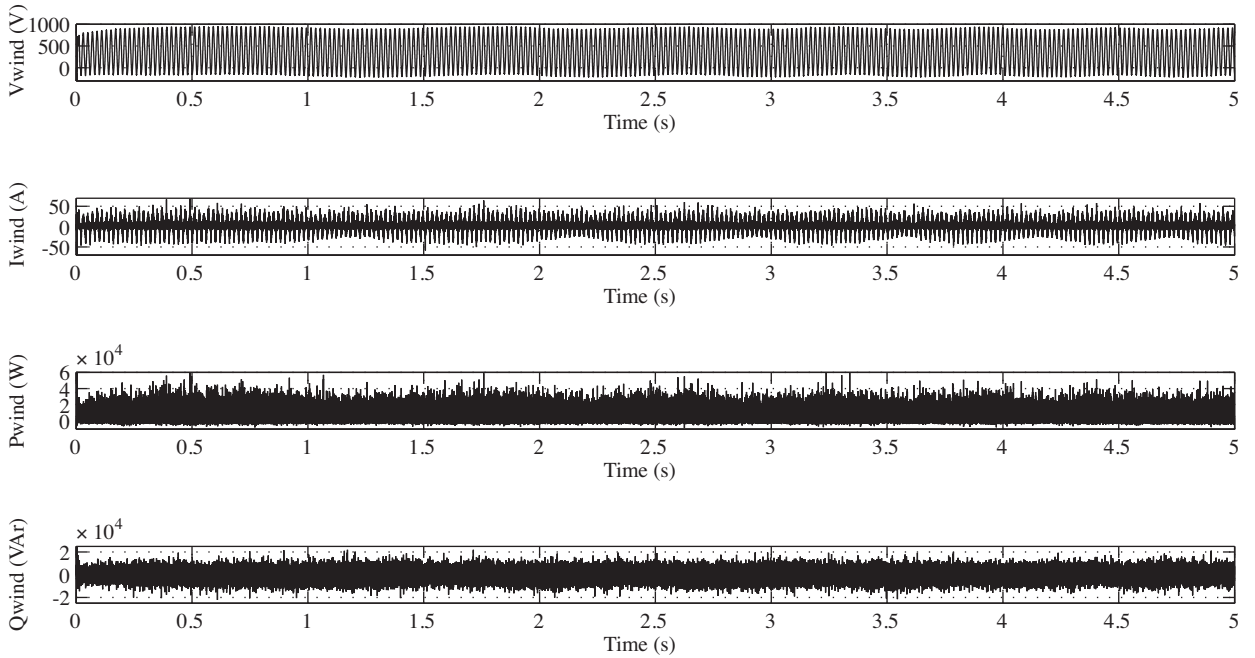


Figure 24. Wind turbine V, I, active, and reactive power variations with FLC system.

5. Conclusion

The waveform of the loads was very similar to the sinus wave form using both the PI and fuzzy logic controllers. The system can fix the voltage on the loads at a constant value of 380 V regardless of effects from the variations of the wind speed. The system frequency value is steady at 50 Hz. According to the value of the wind speed,

the used regulator works effectively by turning on and off the batteries.

The maximum overshoot and settling time values of the FLC were much better than those of the PI controller. The PI controller maximum overshoot voltage that can be reached is 392 V. This value is 384 V with the FLC system. The PI controller's setting time was 2 s; this value was 0.05 s for the FLC.

When the THD values are compared, it is seen that both controllers had values in the standard ranges. However, the FLC's value was better than the PI's, as was its sinus wave form.

When the produced energy is greater and the loads are low, the wind turbine must be arranged to recharge the batteries. This can be done by the management of the energy.

When there is no wind, the loads are supplied only with batteries. When the batteries are empty, the loads will have no energy supply. To prevent this situation, a diesel generator can be added to the system or the system can be supplied with energy by the main network.

References

- [1] J. Peinke, P. Schaumann, S. Barth, Wind Energy Proceedings of the Euromech Colloquium, Berlin-Heidelberg, Springer, 2007.
- [2] Global Wind and Energy Council, Market Forecast 2010-2014, available at: http://www.gwec.net/fileadmin/documents/Publications/Global_Wind_2007_report/market%20forecast%202010-2014.JPG.
- [3] M.R. Patel, Wind and Solar Power Systems, Boca Raton, Florida, CRC Press, 2006.
- [4] T. Ackerman, Wind Power in Power Systems, New York, John Wiley and Sons, 2005.
- [5] P.A. Stott, M.A. Mueller, "Modelling fully variable speed hybrid wind diesel systems", 41st International Universities Power Engineering Conference, Vol. 1, pp. 212-216, 2006.
- [6] A. Karlis, P. Dokopoulos, "Small power systems fed by hydro, photovoltaic, wind turbines and diesel generators", Third IEEE International Conference on Electronics, Circuits, and Systems, Vol. 2, pp. 1013-1016, 1996.
- [7] X. Liu, S. Islam, "Wind-diesel-battery hybrid generation system reliability analysis on site and size factors", 4th International Conference on Electrical and Computer Engineering, pp. 229-232, 2006.
- [8] A.S. Kini, U.R. Yaragatti, "Modelling and simulation of a wind/diesel hybrid power system", IEEE International Conference on Industrial Technology, pp. 1670-1675, 2006.
- [9] Y.M. Chen, Y.C. Liu, S.C. Hung, C.S. Cheng, "Multi-input inverter for grid-connected hybrid PV/wind power system", IEEE Transactions on Power Electronics, Vol. 22, pp. 1070-1077, 2007.
- [10] V. Rao, C. Chinnagounder, "Analysis of hybrid power system", First Asia International Conference on Modelling and Simulation, pp. 48-52, 2007.
- [11] M.J. Khan, M.T. Iqbal, "Analysis of a small wind-hydrogen stand-alone hybrid energy system", Applied Energy, Vol. 86, pp. 2429-2442, 2009.
- [12] H. Miland, R. Glöckner, P. Taylor, R.J. Aaberg, G. Hagen, "Load control of a wind-hydrogen stand-alone power system", International Journal of Hydrogen Energy, Vol. 31, pp. 1215-1235, 2006.

- [13] M.J. Khan, M.T. Iqbal, "Dynamic modeling and simulation of a small wind-fuel cell hybrid energy system", *Renewable Energy*, Vol. 30, pp. 421-439, 2005.
- [14] M.E. Ropp, S. Gonzales, "Development of a MATLAB/Simulink model of a single-phase grid-connected photovoltaic system", *IEEE Transactions on Energy Conversion*, Vol. 24, pp. 195-202, 2009.
- [15] Y.M. Chen, C.S. Cheng, H.C. Wu, "Grid-connected hybrid PV wind power generation system with improved DC bus voltage regulation strategy", 21st Annual IEEE Applied Power Electronics Conference and Exposition, doi: 10.1109/APEC.2006.1620673, 2006.
- [16] Y.M. Chen, S.C. Hung, C.S. Cheng, Y.C. Liu, "Multi-input inverter for grid-connected hybrid PV/wind power system", 20th Annual IEEE Applied Power Electronics Conference and Exposition, Vol. 2, pp. 850-856, 2005.
- [17] B. Lu, M. Shahidehpour, "Short-term scheduling of battery in a grid-connected PV/battery system", *IEEE Transactions on Power Systems*, Vol. 20, pp. 1053-1061, 2005.
- [18] F. Giraud, Z.M. Salameh, "Steady-state performance of a grid-connected rooftop hybrid wind-photovoltaic power system with battery storage", *IEEE Transactions on Energy Conversion*, Vol. 16, pp. 1-7, 2001.
- [19] K. Ro, S. Rahman, "Two-loop controller for maximizing performance of a grid-connected photovoltaic-fuel cell hybrid power plant", *IEEE Transactions on Energy Conversion*, Vol. 13, pp. 276-281, 1998.
- [20] T. Petru, T. Thiringer, "Modeling of wind turbines for power system studies", *IEEE Transactions on Power Systems*, Vol. 17, pp. 1132-1139, 2002.
- [21] T. Wildi, *Electrical Machines, Drives, and Power Systems*, New Jersey, Prentice Hall, 1997.
- [22] L. Krichen, B. Francois, A. Ouali, "A fuzzy logic supervisor for active and reactive power control of a fixed speed wind energy conversion system", *Electric Power Systems Research*, Vol. 78, pp. 418-424, 2008.
- [23] E. Levi, Y.W. Liao, "An experimental investigation of self-excitation in capacitor excited induction generators", *Electric Power Systems Research*, Vol. 53, pp. 59-65, 2000.
- [24] E. Muljadi, J. Sallan, M. Sanz, C.P. Butterfield, "Investigation of self-excited induction generators for wind turbine applications", *Annual Meeting of the IEEE Industry Applications Society*, Vol. 1, pp. 509-515, 1999.
- [25] F. Iov, M. Ciobotaru, D. Sera, R. Teodorescu, F. Blaabjerg, "Power electronics and control of renewable energy systems", 7th International Conference on Power Electronics and Drive Systems, pp. 6-28, 2007.
- [26] S.A. Papathanassiou, G.A. Vokas, M.P. Papadopoulos, "Use of power electronic converters in wind turbines and photovoltaic generators", *IEEE International Symposium on Industrial Electronics*, Vol. 1, pp. 254-259, 1995.
- [27] H. Weiss, J. Xiao, "Fuzzy system control for combined wind and solar power distributed generation unit", *IEEE International Conference on Industrial Technology*, Vol. 2, pp. 1160-1165, 2003.
- [28] O.O. Mengi, I.H. Altas, "A fuzzy logic control for wind/battery renewable energy production system", *International Symposium on Innovations in Intelligent Systems and Applications*, pp. 229-233, 2010.
- [29] A. de Medeiros Torres, F.L.M. Antunes, F.S. dos Reis, "An artificial neural network-based real time maximum power tracking controller for connecting a PV system to the grid", 24th Annual Conference of the IEEE Industrial Electronics Society, Vol. 1, pp. 554-558, 1998.

- [30] O. Tremblay, L.A. Dessaint, A.I. Dekkiche, "A generic battery model for the dynamic simulation of hybrid electric vehicles", Vehicle Power and Propulsion Conference, pp. 284-289, 2007.
- [31] K. Ogata, Modern Control Engineering, 4th ed., New Jersey, Prentice Hall, 2001.
- [32] L.A. Zadeh, "Fuzzy sets", Information Control, Vol. 8, pp. 338-353, 1965.
- [33] L.A. Zadeh, "Applied Soft Computing - foreword", Applied Soft Computing, Vol. 1, pp. 1-2, 2001.